Anharmonic model for polyyne

Michael Springborg
*Nordisk Institut for Teoretisk Atomfysik (NORDITA), Blegdamsvej 17, DK-2100 København Ø, Denmark and Fakultät für Chemie, Universität Konstanz, D-7750 Konstanz, Federal Republic of Germany**

Stefan-Ludwig Drechsler
Zentralinstitut für Festkörperphysik und Werkstofforschung, Akademie der Wissenschaften der Deutschen Demokratischen Republik, Helmholtzstrasse 20, DDR-8027 Dresden, German Democratic Republic

Jiří Málek†
Laboratory of Theoretical Physics, Joint Institute of Nuclear Research, Dubna, P.O. Box 79, 101 000 Moscow, U.S.S.R.
(Received 8 May 1989; revised manuscript received 18 December 1989)

With use of the first-principles, density-functional, full-potential, linear muffin-tin orbital (LMTO) method for helical polymers, calculations on carbon chains have been carried through. The results are used in providing parameters for model Hamiltonians related to the well-known Su-Schrieffer-Heeger model for sp^2-bonded conjugated polymers. However, the lattice part (H_σ) is found to contain strong anharmonic contributions. Using the models solitons, polarons, and "twistons" are examined. Due to the anharmonicity, polaronic states are energetically favored compared with solitonic states. Moreover, a rich variety of (meta)stable polarons is found. It is argued that the ground state of the charged system is a polaron lattice. Finally, twistons are found to be unstable when interchain couplings are neglected.

I. INTRODUCTION

Since it was discovered[1] that upon doping *trans*-polyacetylene increases its conductivity by very many orders of magnitude, efforts for an understanding of this phenomenon and the search for other conjugated polymers with similar properties have increased enormously (see, e.g., Refs. 2–4). Almost all the polymers that in this context have been considered contain a (almost) planar carbon backbone. The bonds between neighboring carbon atoms are formed by σ orbitals constructed from sp^2 hybrids and by π orbitals from p orbitals perpendicular to the plane of the carbon nuclei. For most of these systems the ground state has alternating single and double carbon-carbon bonds. The two structures with different patterns of alternating bond orders have comparable total energy, and for certain conjugated polymers with high symmetry they become degenerate. The doping-induced conducting properties of these polymers are often ascribed solitons which are domain walls separating parts of the polymer chain with different bond order patterns or polarons which separate similar bond order patterns (see, e.g., Refs. 2–7).

The starting point of many theoretical examinations of both the ground state and the low-energy excited states is the Su-Schrieffer-Heeger (SSH) model Hamiltonian.[8,9] In the static version of this model (i.e., neglecting kinetic-energy terms of the nuclei) it is assumed that the total energy can be written as a tight-binding part of the carbon π electrons plus a remaining repulsive term. The latter is to lowest order in the carbon-carbon interatomic distances written as a sum of harmonic terms, and an electron-phonon coupling is included in the tight-binding part by making the hopping integrals depend on the bond lengths. The model—developed for *trans*-polyacetylene but often applied also on other conjugated polymers—includes only the carbon π electrons explicitly and assumes all other occupied electronic levels to have such low energies that the effects of those can be incorporated in the harmonic terms. The positions of the carbon atoms are described by the parameters $\{u_n\}$. u_n is the position of the nth carbon atom on an axis perpendicular to the bisector of the carbon bond angle for this atom relative to its position in the perfect undimerized polymer. For the perfect dimerized polymer, $u_n=(-1)^n u_0$ and the ground state is found for a certain value of $u_0 \equiv u_{(0)} \neq 0$.

The simplest conjugated polymer one can think of is a linear carbon chain. The existence of such chains has been reported both by Kasatochkin *et al.*[10] and by Akagi *et al.*[11] although it has been argued[12] that because of its much smaller valence-band width compared with that of two- and three-dimensional carbon (graphite and diamond, respectively) one should expect it to be only metastable. This compound has the advantage that it can be considered a simple and highly symmetric prototype of conjugated polymers and it has therefore been the subject of some recent attention.[11–17] Moreover, Akagi *et al.*[11] have reported a doping-induced enhancement of the electrical conductivity of 7 orders of magnitude similar to that reported for other conjugated polymers.

In contrast to most other conjugated polymers, the undimerized chain consists of carbon-carbon double bonds whereas the dimerized chain has alternating single and triple bonds. Due to the full rotational symmetry of the chains, the effective internal π electron degeneracy is 4 not 2 as for most other conjugated polymers, when in-

cluding spin degeneracy. Hence, a remarkably rich variety of nonlinear excited states including solitons, polarons, polarexcitons, and breathers has been predicted by Rice *et al.*[13] However, all quantities were examined using the simplest SSH model and because of the lack of proper parameter values those of *trans*-polyacetylene were used. It is therefore one purpose of the present paper to consider explicitly the carbon chains. From self-consistent first-principles calculations on the ground state of a number of geometries we will derive parameters for a model Hamiltonian and afterwards apply the model Hamiltonian to examine some symmetry-breaking solitonic and polaronic distortions.

The existence of so-called "twistons" in sp^2-bonded conjugated polymers has recently been proposed.[18] A twiston is a distortion for which a smaller part of the polymer backbone is lifted out of the common plane, and it can thus qualitatively be considered a distortion where the two dimensionality of the nuclear backbone locally has been changed into true three dimensionality. Due to the one dimensionality of the carbon chains the equivalent "twistonic" excitations would lead to a local two-dimensionality of the backbone. Here, more types of geometries can be proposed of which the two simplest ones are one with a local zigzag arrangement and one with a local bent arrangement (for more precise definitions, see later). These excitations will split the doubly degenerate π states into singly degenerate σ and π states. It is interesting to notice that when keeping all bond lengths constant the energies of these excitations are expected to be small, since they will mainly be determined from small variations in the nearest-neighbor and next-nearest-neighbor interactions. Although the stability of twistons is assumed caused by interchain couplings,[18] we will here analyze a twistonic defect in a single, isolated carbon chain, believing that without understanding this it is not possible to understand the twistonic defects in a multichain environment. From first-principles calculations on zigzag carbon chains we will therefore derive a model Hamiltonian, which we will use in examining the twistons.

The paper is organized as follows. In Sec. II we give a brief account of the first-principles method for calculating the electronic ground state of a single polymer. For a more detailed description the reader is referred to Refs. 19 and 20. Section III contains the results of the first-principles calculations, and in Sec. IV we examine the solitonic, polaronic, and twistonic defects. We conclude in Sec. V.

II. THE FIRST-PRINCIPLES METHOD

The first-principles method has been described in detail elsewhere,[19,20] but we will give here a brief introduction.

Within the Hohenberg-Kohn density-functional formalism[21–23] the problem of calculating the electronic ground state of a given system with fixed nuclear positions is reduced to that of solving the single-particle Kohn-Sham equations (in Rydberg atomic units),

$$[-\nabla^2+V(\mathbf{r})]\phi_i(\mathbf{r})=\varepsilon_i\phi_i(\mathbf{r}) \ . \tag{1}$$

$V(\mathbf{r})$ is the sum of the Coulombic potential of the nuclei, $V_N(\mathbf{r})$, that of the electronic density, $V_e(\mathbf{r})$, and the remaining so-called exchange-correlation potential $V_{\rm xc}(\mathbf{r})$. The latter we approximate using the local approximation of von Barth and Hedin.[24] Then, $V_e(\mathbf{r})$ and $V_{\rm xc}(\mathbf{r})$ are both simple functionals of the electron density

$$\rho(\mathbf{r})=\sum_i |\phi_i(\mathbf{r})|^2 \ , \tag{2}$$

where the summation runs over all occupied orbitals. Accordingly, Eqs. (1) and (2) are to be solved self-consistently.

The single-particle eigenfunctions $\phi_i(\mathbf{r})$ are expanded in linear muffin-tin orbitals (LMTO's) which are defined as follows. Inside nonoverlapping (muffin-tin) spheres centered on the nuclei, Eq. (1) with $V(\mathbf{r})$ replaced by its spherically symmetric component can be solved numerically for a reasonable choice of ε_i (i.e., in the middle of the region for which that particular function is of importance). The resulting functions are matched smoothly to spherical Hankel functions, $h_l^{(1)}(\kappa r)Y_{lm}(\hat{\mathbf{r}})$, $\kappa^2<0$. A function centered on one site is inside any other sphere augmented continuously and differentiably with the numerical functions of that sphere. The basis functions are accordingly eigenfunctions to a muffin-tin potential, but it should be stressed that everywhere else the *full* potential is considered. We use two subsets of basis functions, each defined by one common κ for all atoms and (l,m)'s. The κ's and the sphere radii are kept constant throughout all sets of calculations.

In the present work we have applied the method on a single, isolated, linear or zigzag, periodic, infinite carbon chain with two atoms per unit cell. The radii of the muffin-tin spheres were set to 1.1 a.u. and the two values of the decay constants, κ, to $0.7i$ and $1.5i$, respectively. s, p, and d functions were included in the basis set but because of almost linear dependences of the basis functions the set had to be contracted, and the size was then reduced from 36 to 32 functions per unit cell. The continuous k variable was replaced by n_k equidistant points in the interval $[0,\pi/D]$, D being the length of the unit cell. 0 as well as π/D were included in the k set. Except where otherwise mentioned, we used $n_k=6$.

The method has earlier been applied successfully on other systems including linear carbon chains[12] and the most well-known conjugated polymer, polyacetylene.[25–27] The purpose of the earlier paper on linear carbon chains was to demonstrate the feasibility of the first-principles method for helical polymers. Accordingly, the examined geometries in that work were characterized by large variations in the bond lengths, and from a fairly crude mesh estimates of the optimum values of the bond lengths for both the undimerized and the dimerized isomers were obtained. In the present paper we will examine the dimerization in detail. Thus, we do not attempt to optimize any bond length but will consider some paths in the two-dimensional configuration space in detail for the linear chains. It should, however, be pointed out that compared with the previous report[12] the quality of the calculations was improved (i.e., the numbers of neigh-

bors and of basis functions were increased).

In order to obtain parameters for the model Hamiltonian for the twistons we have also considered zigzag geometries where the bond angles deviated from 180° keeping the bond lengths fixed.

We would like to point out that although there is no formal correspondence between the single-particle energies ε_i calculated within the density-functional formalism and the electronic excitations energies, experience has shown that it is a good approximation to neglect this formal inconsistency, and this will accordingly be done here.

III. THE FIRST-PRINCIPLES RESULTS

A. Linear chains

We performed three sets of first-principles calculations for linear carbon chains. In the first set the unit-length was kept fixed at $D=5.06$ a.u., which is the average between the earlier reported[12] optimized values for undimerized and dimerized carbon chains. By varying the dimerization (i.e., the difference of the lengths of the two nearest-neighbor bonds $\Delta d \equiv d_{+1}-d_{-1}$) we found [cf. Fig. 1 (a)] the lowest total energy for $\Delta d=0.34$ a.u., cor-

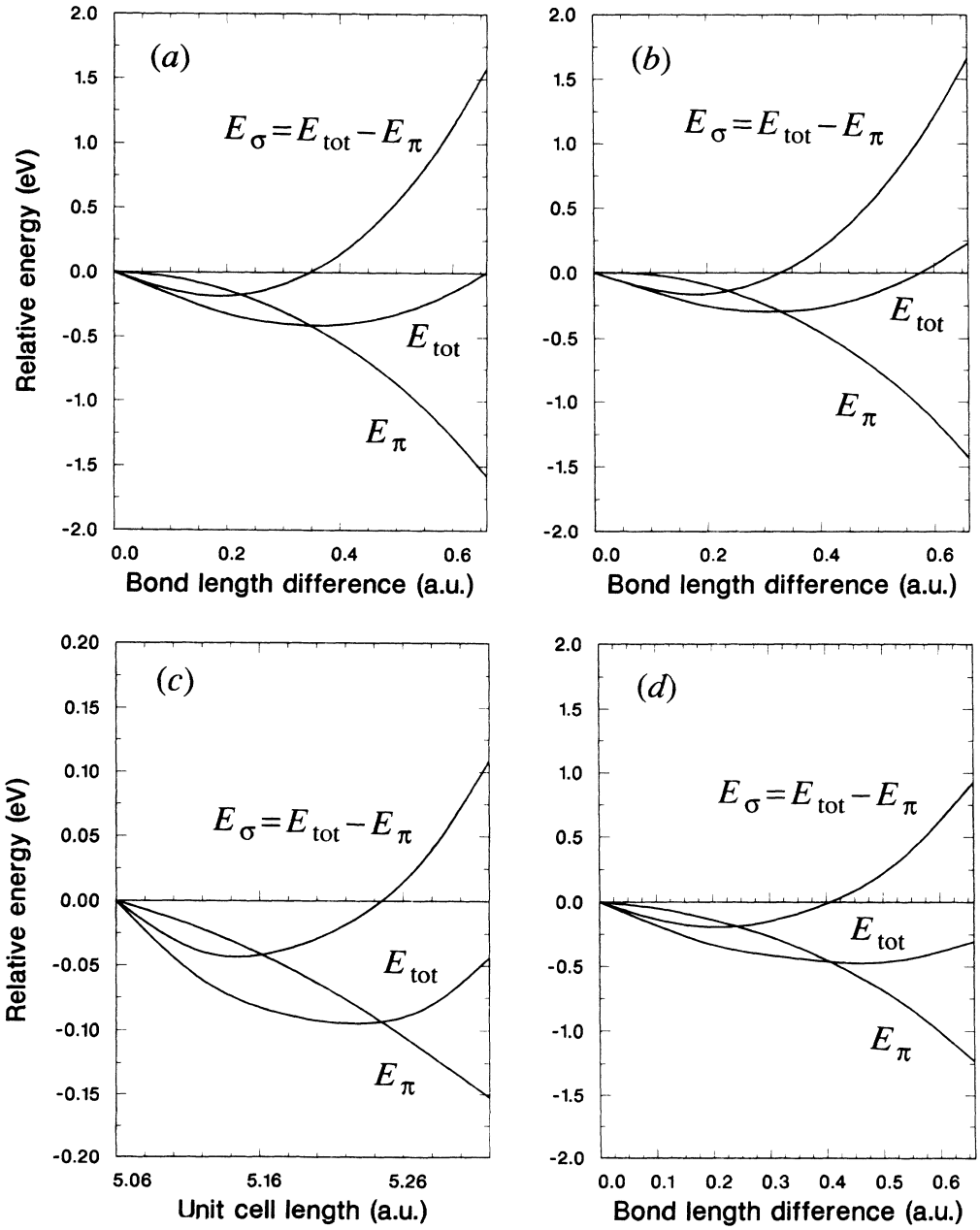

FIG. 1. The relative total energy E_{tot}, the π electron energy E_π, defined as the integral over the Brillouin zone of the π electron single-particle valence energies, and the difference $E_\sigma \equiv E_{tot} - E_\pi$. The energies are shown in eV per C_2 unit for the linear chain for various paths in the two-dimensional configuration space defined by the two bond lengths d_{-1} and d_{+1}. In (a) and (b), $d_{+1}+d_{-1}=5.06$ a.u., in (c) we have $d_{-1}-d_{+1}=0.34$ a.u., whereas in (d) $d_{+1}+d_{-1}=5.22$ a.u. (a), (c), and (d) have been obtained using six k points in half part of the Brillouin zone, whereas (b) shows estimated curves in the limit of an infinite number of k points.

responding to bond lengths $d_{+1}=2.70$ a.u. and $d_{-1}=2.36$ a.u. In the second set we kept this value of the bond-length difference $\Delta d=0.34$ a.u. and varied the unit-cell length ($D=d_{+1}+d_{-1}$). In this set the lowest total energy was found [cf. Fig. 1(c)] for $D=5.22$ a.u. In the last set we then fixed D at this value (5.22 a.u.) and varied Δd, obtaining an optimized value [cf. Fig. 1(d)] of $\Delta d=0.46$ a.u., i.e., $d_{+1}=2.84$ a.u. and $d_{-1}=2.38$ a.u.

The three sets do not represent any attempt of optimizing the bond lengths but were merely carried through in order to have detailed information about the band structures and the total energies for a number of realistic geometries. It is nevertheless worthwhile to compare the bond lengths with those obtained in a few other attempts of calculating carbon-carbon bond lengths of conjugated polymers.

Ab initio Hartree-Fock calculations on carbon chains[28–31] have predicted bond-length differences of $\Delta d=0.28-0.50$ a.u., whereas recent semiempirical Hartree-Fock calculations[32] predicted 0.31 a.u. These values agree well with the present ones as well as with the earlier results (0.36 a.u.; Ref. 12), and our present results indicate therefore that we can describe the dimerization of a conjugated polymer realistically. On the other hand, the Hartree-Fock approach usually underestimates bond lengths, thereby explaining the smaller values of D found in the *ab initio* calculations (4.64–4.89 a.u.; Refs. 28–31) and in the semiempirical calculations (4.94 a.u.; Ref. 32), whereas our approach often overestimates the bond lengths.

Density-functional calculations on *trans*-polyacetylene have recently been reported by Ashkenazi *et al.*[33] Based upon their finding of an optimized structure with (almost) vanishing dimerization, they suggested that a Peierls mechanism cannot describe the dimerization of this system. The carbon chains have so many properties in common with *trans*-polyacetylene that one might expect similar effects to show up for the carbon chains. However, the results of Ashkenazi *et al.* might be questioned, since other density-functional calculations on *trans*-polyacetylene[25,26,34–41] have predicted nonvanishing bond-length alternation. For later reference we mention in particular the calculations by Mintmire and White.[37,38] They demonstrated that as a function of an increasing number of equidistant k points (n_k) used in describing the continuous k variable, the dimerization amplitude will decrease, but also in the limit $n_k\to\infty$ it is found to be nonvanishing.

The Hartree-Fock calculations on *trans*-polyacetylene[42–53] have predicted dimerization amplitudes in reasonable agreement with the experimental values.[54,55] Of most relevance here are the results of Suhai[47,48] and of Brédas *et al.*[50] Suhai reported that when adding correlation effects perturbatively to results of an *ab initio* Hartree-Fock calculation the optimized dimerization amplitude will decrease. This decrease amounts to about 20% when about 75% of the total correlation effects are included. On the other hand, the semiempirical PPP (Pariser-Parr-Pople) calculations by Brédas *et al.* predicted that the optimized dimerization amplitude would increase upon inclusion of correlation effects.

In total, the surprising finding by Ashkenazi *et al.*[33] does not seem to be confirmed by any other parameter-free approach. Neither other density-functional calculations with a local approximation for correlation effects, nor Hartree-Fock calculations without correlation, nor calculations with nonlocal treatments of correlation effects have yielded vanishing dimerization amplitude. Therefore, we consider the results of Fig. 1 to be representative of those obtained using parameter-free descriptions of conjugated polymers in contrast to those of Ashkenazi *et al.* It should finally be mentioned that Ashkenazi *et al.* find the total energy as a function of the dimerization amplitude to have a nonzero slope for zero dimerization. Although our curves in Fig. 1 might seem to indicate a similar behavior we find it beyond our numerical accuracy to confirm or disprove this.

The dimerization energies (i.e., the difference in the total energy for the undimerized and the dimerized chain) are here found to be about 0.5 eV per C_2 unit. *Ab initio* Hartree-Fock calculations by Kertész *et al.*[28] have yielded values larger than 1 eV per C_2 unit, whereas those of Karpfen[30] gave 0.3 eV per C_2 unit. Our values thus qualitatively agree with those reported earlier.

We now return to the first-principles results of Fig. 1 and relate them to a model Hamiltonian with which solitons and polarons will be studied in the next section.

Since the band structures (see, e.g., Ref. 12) separate completely into π bands closest to the Fermi level and σ bands more far away, it is a good approximation to only describe the π electrons accurately, as is the case in the SSH model. We will extend the SSH model by describing the π electrons with a tight-binding Hamiltonian including as well on-site terms as next-nearest-neighbor interactions:

$$H_\pi=\sum_{n,s}\left[\varepsilon_n c_{n,s}^\dagger c_{n,s} - \sum_{m=1}^{2} t_{n+m,n}(c_{n+m,s}^\dagger c_{n,s}+c_{n,s}^\dagger c_{n+m,s})\right] . \tag{3}$$

Here, $c_{n,s}^\dagger$ ($c_{n,s}$) creates (annihilates) a π electron on site n of type s, where s labels both spin and p_x or p_y orbital. The polymer is assumed parallel to the z axis.

The hopping integrals t are linearized in bond lengths:

$$t_{n+m,n}=t_m^0-\alpha_m(d_{n+m,n}-d_m) , \tag{4}$$

where d_m is a typical mth-nearest-neighbor distance.

The on-site terms ε_n are assumed being a sum of a constant (which in the present context in unimportant) and in "ionicity" term. The existence of the latter can be understood as follows: Each carbon atom prefers being fourfold coordinated, which for the present linear chains means that the sum of the bond orders of the two nearest-neighbor bonds for any carbon atom should be close to 4. Therefore, an atom for which the two nearest-neighbor bonds are elongated (shortened) will attract (repel) extra electrons. By linearizing in bond lengths we arrive at

$$\varepsilon_n=\varepsilon_0^0-\zeta(d_{n+1,n}+d_{n,n-1}-2d_1) . \tag{5}$$

In the first and third set of calculations we fixed D. Choosing in each set $d_m = md_1$ and $d_1 = D/2$ we fitted the first-principles π valence bands obtained in all calculations of a specific set with the energies predicted by Eq. (3), thereby obtaining t_1^0, α_1, and t_2^0. We found $t_1^0 = 2.43$ eV, $\alpha_1 = 4.42$ eV/Å, and $t_2^0 = -0.12$ eV in the first set, and $t_1^0 = 2.19$ eV, $\alpha_1 = 3.88$ eV/Å, and $t_2^0 = -0.09$ eV in the third set. The decrease in the values from the first set to the third set is due to the increased unit-cell length. The values of the nearest-neighbor hopping integrals are comparable to those used for *trans*-polyacetylene by Su, Schrieffer, and Heeger,[8,9] and slightly smaller than those obtained from first-principles calculations on polyacetylene.[25,26] The next-nearest-neighbor interactions are, on the other hand, considerably smaller than those for *trans*-polyacetylene.[25,26] This is due to large interatomic distances and to a more complete "screening" from nearest neighbors.

According to the tight-binding model the gap between π valence and conduction bands varies linearly as a function of Δd with the coefficient $2\alpha_1$, which becomes 8.8 eV/Å in the first set and 7.8 eV/Å in the third set. According to the first-principles calculations, the slope is 10.5 and 10.0 eV/Å. It is surprising that the model predicts a smaller gap than the first-principles calculation, since density-functional local-density calculations usually underestimate the gap. Both the models and the first-principles calculations predict a gap of about 2 eV for the ground state, in good agreement with the data by Akagi *et al.*[11] These results taken together indicate that we have overestimated the bond-length alternation, especially in the third set of calculations. It should be added that compared with our earlier report[12] the calculations have been improved by including more basis functions and interactions with more distant neighbors. These improvements have led to a reduction in the gap, and one might speculate that even further improvements would lead to further reductions. We have not examined this point in detail, but we believe the effects to be relatively small.

The results of the second set of calculations can be used in estimating α_2 and ζ. By choosing half the unit-cell length of the first set of calculations as typical carbon-carbon bond lengths (i.e., $d_1 = 2.53$ a.u., $d_m = md_1$), we found by fitting the π valence bands $t_1^0 = 3.12$ eV, $\alpha_1 = 3.85$ eV/Å, $t_2^0 = -0.34$ eV, $\alpha_2 = -1.13$ eV/Å, and $\zeta = 4.78$ eV/Å. Compared with the values of the first set we notice some modifications, but the agreement is reasonable. When fixing $\zeta = 0$ (i.e., neglecting the "ionicity" term) the fit became significantly worse.

In all fits the root mean squares of deviations were smaller than 0.1 eV. This value should be compared with, e.g., the π valence-band width, i.e., 4–5 eV.

By summing the single-particle π valence energies of the first-principles calculations over the same k points as used in obtaining the total energies E_{tot} of Fig. 1, we obtain the π energy, E_π, shown in Fig. 1 The difference is the so-called σ energy: $E_\sigma \equiv E_{\text{tot}} - E_\pi$, and this is also shown in Fig. 1. In the first and third set of calculations we see that E_π has a maximum for vanishing bond-length alternation, as is also the case in the SSH mode., but E_σ is not a parabola with minimum for $\Delta d = 0$, as is assumed in the SSH model. This means that a harmonic approximation for E_σ is not justified and one has to use an anharmonic potential. Since the variations in the energies of Fig. 1(c) are 1 order of magnitude smaller than those of Figs 1(a) and 1(d), we will concentrate on describing E_σ of the latter. For these we may use

$$E_\sigma = \tfrac{1}{2}K[(\tfrac{1}{2}\Delta d - x_s)^2 - x_s^2] \,. \tag{6}$$

Reasonable values are $K = 80$ eV/Å^2 and $x_s = 0.05$ Å.

As mentioned above, Mintmire and White[37,38] have argued that replacing the continuous k variable with a finite equidistant mesh leads to an overestimate in the dimerization energy and amplitude due to improper treatment of the π bands. We repeated the calculations of the first set for $\Delta d = 0$ and $\Delta d = 0.34$ a.u. for $n_k = 2$, 3, 6, 11, 16, and 21 equally spaced k points in half part of the first Brillouin zone. We then assumed that

$$E_x(\Delta d) - E_x(0) = E_x^\infty(\Delta d) + a_x \, \Delta d \, \exp(-n_k b) \tag{7}$$

with E_x being either the total energy (E_{tot}) or the π energy (E_π). Thus, we assume the relative error due to finite n_k to depend linearly upon dimerization amplitude and exponentially upon n_k. These assumptions led to the curves of Fig. 1(b) replacing those of Fig. 1(a) in the limit $n_k \to \infty$. We see that the optimized dimerization amplitude is slightly decreased and the dimerization energy is decreased more. In agreement with the findings of Mintmire and White, E_σ is only slightly affected. It should finally be stressed that Fig. 1(b) merely represents an attempt of estimating the results for $n_k \to \infty$.

For *trans*-polyacetylene one of us has recently examined the effect of dimerization[25,26] by following a special

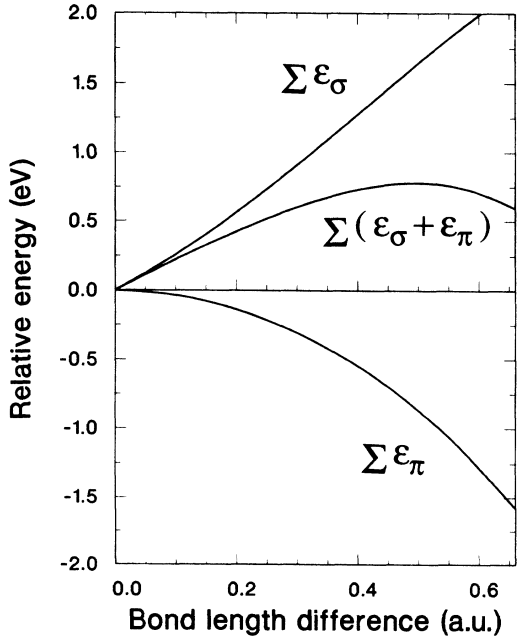

FIG. 2. The integral over the Brillouin zone of the single-particle energies separated in π and σ contributions for the same geometries as in Fig. 1(a).

path in configuration space. In this path the length of the unit cells was slightly increased as a function of increasing bond-length difference. It turned out that both the total energy and the sum of the quasiparticle energies of the occupied (σ as well as π) valence orbitals possessed a minimum for a nonzero dimerization. In Fig. 2 we depict similarly the sum of the energies of the valence levels and split it into a σ and a π part for the calculations of the first path [cf. Fig. 1(a)]. Comparing with the results of *trans*-polyacetylene (Refs. 26 and 27) we see that the situation is different: the σ and the π part have both extrema for $\Delta d=0$, and we therefore suggest that the results for *trans*-polyacetylene were affected by the special path in which the unit-cell length was not kept constant. There, as a function of increasing bond-length alternation, the shorter bond lengths decreased more slowly than the longer bond lengths increased. In the present calculations the bond lengths change at the same rate.

B. Zigzag chains

In the last set of calculations—which we will use later when examining the twistons—we fixed the bond lengths at the values for the minimum of the total energy in Fig. 1(d), i.e., $d_1=2.38$ a.u. and $d_2=2.84$ a.u. We lowered the symmetry of the chain by varying the bond angle θ from 180° (the value for the linear chain) to 140°. In this case the doubly degenerate π bands of the linear chains split up into a σ and a π band. The calculated valence-band energies and total energies are shown in Fig. 3.

In the figure we notice a small tendency for the system to leave the linear symmetry and possess a zigzag geometry. However, the energy differences are so small that we cannot conclude definitively that this is the case. We furthermore notice that both integrated single-particle energies possess a minimum for a bond angle different from 180°. The minimum is around 155° for the π band and around 168° for the σ band. Compared with Fig. 1 the energies of Fig. 3(a) as functions of the geometrical parameter show a more complicated dependence.

For each of the two upper valence bands we assume a tight-binding description. By leaving the linear symmetry, the characters of the electronic levels change. For the band which becomes of σ character for the zigzag structure the s-component increases continuously from 0 for $\theta=180°$. This change will be related to a change in the on-site matrix elements and can be estimated from the relative position of the σ band as a function of θ. This (defined as the average of the top and the bottom of the band) is shown in Fig. 3(b) together with the bandwidth for both the σ and the π band. As is seen also, the position of the π band changes as a function of θ. We notice that the relative positions of the bands closely follow the integrated energies. By neglecting next-nearest-neighbor interactions (which were found to be small in the previous sets of calculations) the width and the position of the valence band is $2\times\max\{|t_{+1}|,|t_{-1}|\}$ and $\min\{|t_{+1}|,|t_{-1}|\}$, respectively. A model that *qualitatively* describes the tendencies of Fig. 3 is then (assuming $|t_{+1}|>|t_{-1}|$)

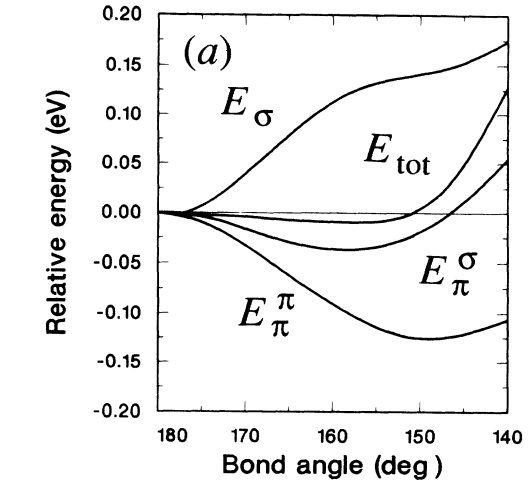

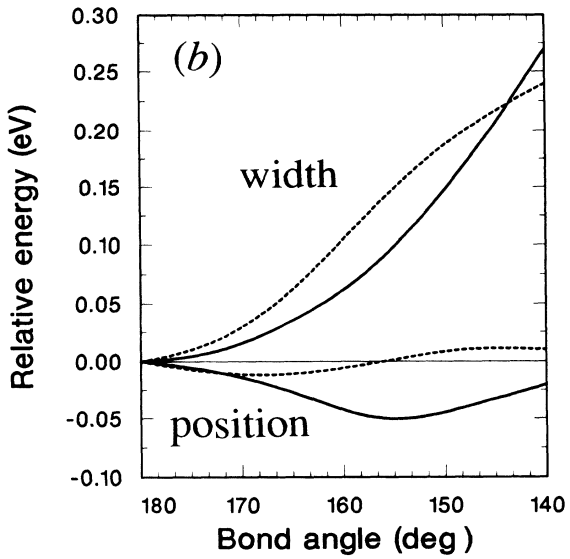

FIG. 3. (a) The relative total energy E_{tot}, the π electron energies E_π^π and E_π^σ, and the remainder E_σ for a zigzag carbon chain as functions of the carbon bond angle α for α varying from 180° (corresponding to the linear structure) to 140°. E_π^π and E_π^σ are defined as the integral over the Brillouin zone of the π energy band and the uppermost (π-derived) σ band, respectively. E_σ is defined as the difference $E_{tot}-E_\pi^\pi-E_\pi^\sigma$. The energies are in eV per C_2 unit and have been obtained with six k points in half part of the Brillouin zone. (b) The relative widths and the relative positions of the electronic energy bands as a function of α. The latter is defined as the average of the position of the top and the bottom of the valence band. The solid (dashed) curves correspond to the $\pi(\sigma)$ band.

$$
\begin{aligned}
t_{-1}^{\sigma} &= t_{-1}^{0\sigma} + 4\times10^{-5}(\theta-180°)^2 \text{ eV/deg}^2 , \\
t_{-1}^{\pi} &= t_{-1}^{0\pi} + 4\times10^{-5}(\theta-180°)^2 \text{ eV/deg}^2 , \\
t_{+1}^{\sigma} &= t_{+1}^{0\sigma} + 0.01\left[\cos\left[\frac{180°-\theta}{12°}\times180°\right]-1\right] \text{ eV} , \\
t_{+1}^{\pi} &= t_{+1}^{0\pi} + 0.03\left[\cos\left[\frac{180°-\theta}{25°}\times180°\right]-1\right] \text{ eV} ,
\end{aligned}
\tag{8}
$$

whereas the next-nearest-neighbor interactions are set to zero:

$$t^{\sigma}_{\pm 2}=t^{\pi}_{\pm 2}=0 \ . \tag{9}$$

For small deviations of the bond angle from 180° we can write the rest of the total energy approximately as

$$E_{\sigma}=5\times 10^{-4}(\theta-180°)^2 \ \text{eV/deg}^2 \ . \tag{10}$$

We would like to point out that the parameters just described are to be considered very approximative. On the other hand, for the purpose of examining the properties of the symmetry-breaking excitations where the bond angles are assumed deviate from 180° in a smaller region the parameters are acceptable.

IV. THE MODEL CALCULATIONS

A. Linear chains

In the model calculations for the linear chains we assume the chain to have fixed length. As Su, Schrieffer, and Heeger, we introduce configuration coordinates u_n such that u_n is the displacement parallel to the polymer axis of the nth carbon atom relative to the position for the perfect, periodic, undimerized chain. The lowest total energy for the neutral chain is then found for $u_n=(-1)^n u_{(0)}$. We will describe the π electrons with H_{π} of Eq. (3) and the bond lengths in Eqs. (4) and (5) are replaced by

$$d_{n+m,n}-d_m=u_{n+m}-u_n \ . \tag{11}$$

The σ energy is included via

$$H_{\sigma}=\tfrac{1}{2}K\sum_n(|u_{n+1}-u_n|-x_s)^2 \tag{12}$$

such that the total Hamiltonian becomes

$$H=H_{\pi}+H_{\sigma} \ . \tag{13}$$

The parameters were chosen according to the third set of calculations of Sec. III A. This includes the approximation of neglecting α_2 and ζ. Although other realistic parameter sets might be chosen (e.g., as obtained for another fixed unit-cell length), the results of Fig. 1 indicate that the modifications in the results will be minor.

We have modeled the infinite polymer by a ring of $N=200$ atoms thereby imposing periodic boundary conditions and avoiding end effects. In performing the model calculations we used two different approaches. In the first "variational" approach we make a simple ansatz of the configuration coordinates [e.g., $u_n=(-1)^n u_{(0)}\tanh(n/L)$ for a soliton] and by varying certain parameters describing the functional form of the ansatz (L in the example) the structure with the lowest total energy is found.

The second "self-consistent" approach has been described in some detail in Ref. 15. In this approach the configuration coordinates u_n are automatically found for structures with local extrema in the total energy once the population of the electronic levels is defined. In Ref. 15 the method was described in detail when H_{σ} was assumed harmonic and here we will only give the equations to be solved in the present anharmonic case.

We define

$$\begin{aligned} v_n&=\frac{\alpha_1}{t_1}(u_{n+1}-u_n) \ , \\ v_s&=\alpha_1 x_s/t_1 \ , \\ f(n)&=P_{n+1,n}+\alpha(P_{n,n+2}+P_{n+1,n-1}) \ , \\ \alpha&=\alpha_2/\alpha_1 \ , \\ P_{n_1,n_2}&=\sum_{\mu=1}^{\text{occ}}\Psi^*_{\mu}(n_1)\Psi_{\mu}(n_2) \ . \end{aligned} \tag{14}$$

Here, $\Psi_{\mu}(n)$ is the coefficient of the μth eigenfunction to the basis function on site n.

The self-consistent conditions are then

$$v_n=v_s\,\text{sgn}(v_n)+\frac{\alpha_1^2}{Kt_1}\{\Lambda-2\ \text{Re}[f(n)]\} \ , \tag{15}$$

where the Lagrange multiplier Λ has been introduced in order to fulfill the fixed-length constraint

$$\sum_n v_n=0 \tag{16}$$

and has the form

$$\Lambda=\frac{2}{N}\sum_{n=1}^{N}\text{Re}[f(n)]-\frac{v_s K t_1}{\alpha_1^2 N}\sum_{n=1}^{N}\text{sgn}(v_n) \ . \tag{17}$$

It should be stressed that the variational and the self-consistent approach need not give identical results. The variational approach requires an ansatz of the configuration coordinates, and only when a realistic one is used is this approach useful. For example, for a soliton one would assume a hyperbolic-tangent shape as is the exact solution in the continuum limit (i.e., when the width of the soliton is much larger that the interatomic spacing) and when H_{σ} is assumed harmonic. Thereby the deviations from hyperbolic-tangent shape will give information on discrete-lattice and anharmonic effects in this case.

1. The perfect chain

In the first set of calculations we fixed the configuration coordinates as

$$u_n=(-1)^n u_0 \tag{18}$$

using the variational approach. By varying u_0 we found the lowest total energy for the neutral polymer for $u_0=u_{(0)}=0.0481$ Å, and by comparing the total energy for this value with that for u_0 the dimerization energy was found to be $E_{\text{dim}}=0.23$ eV per C atom. Both values fit well with those of the first-principles calculations.

The self-consistent approach gives for the configuration coordinates of Eq. (18)

$$y=v_s+\lambda_{\text{eff}}yD[(1-y^2)^{1/2}]\ ,$$
$$y=-\frac{2\alpha_1}{t_1}u_0\ ,$$
$$\lambda_{\text{eff}}=\frac{8\alpha_1^2}{\pi K t_1}\ , \tag{19}$$
$$D(x)=[K(x)-E(x)]/x^2\ ,$$
$$E_{\text{dim}}=\frac{8t_1}{\pi}\{E[(1-y^2)^{1/2}]-1\}+2Ku_0(x_s-u_0)\ ,$$

where $K(x)$ and $E(x)$ denote the complete elliptical integral of first and second kind, respectively. With our parameters we get $u_0=u_{(0)}=0.048$ Å and $E_{\text{dim}}=0.223$ eV per C atom in good agreement with the values of the variational approach.

Rice *et al.*[13,14] have examined in two papers a similar model, which, however, did not contain next-nearest-neighbor interactions in H_π or the anharmonic part of H_σ. Lacking proper values for the remaining parameters they used typical values for *trans*-polyacetylene, i.e., $t_1=3$ eV, $\alpha_1=8$ eV/Å, $K=68$ eV/Å^2, and $x_s=0$. This gave an optimum value of u_0 for the perfect undistorted chain of $u_{(0)}=0.078$ Å in the continuum limit, whereas a numerical treatment of a finite large discrete chain led to $u_{(0)}=0.093$ Å. The optical gap was in the two approaches calculated to be 5 and 5.88 eV, respectively. However, using their parameters extended with next-nearest-neighbor interactions ($t_2=0.3$ eV and $\alpha_2=0.8$ eV/Å; these do not influence the gap or the optimal value of u_0) and for a discrete chain two of us have obtained slightly larger values; i.e., a gap of 6.07 eV and an optimized value of u_0 of $u_{(0)}=0.0948$ Å. It should be pointed out that these values of the gap are 3 to 4 times larger than that reported by Akagi *et al.*[11] and than that of the present study.

2. Solitons

In examining the solitons we used both approaches. In the variational approach we assumed that u_n would follow a hyperbolic-tangent curve and considered, therefore, configurations of the form

$$u_n=(-1)^n u_{(0)}\tanh\left[\frac{n+d-f}{L}\right]\tanh\left[\frac{n+d+f}{L}\right]\ , \tag{20}$$

which is the exact form in the harmonic continuum limit of a soliton-antisoliton pair.[56] By setting $f=N/4$ the pair becomes well separated. Varying d from 0 to 1 and for each value optimize L the mobility of the soliton can be analyzed. It turned out that for fixed d the optimized value of L was (almost) independent of the charge Q of the polymer for $|Q|\leq 2$. L was found to vary between 0.75 for $d=0.0$ and 1.25 for $d=0.5$.

With the self-consistent approach the lowest total energy for a polymer with a solitonlike defect was found for a defect centered on a site; i.e., $d=0.0$ in the language of Eq. (20). In Fig. 4(a) we show the calculated

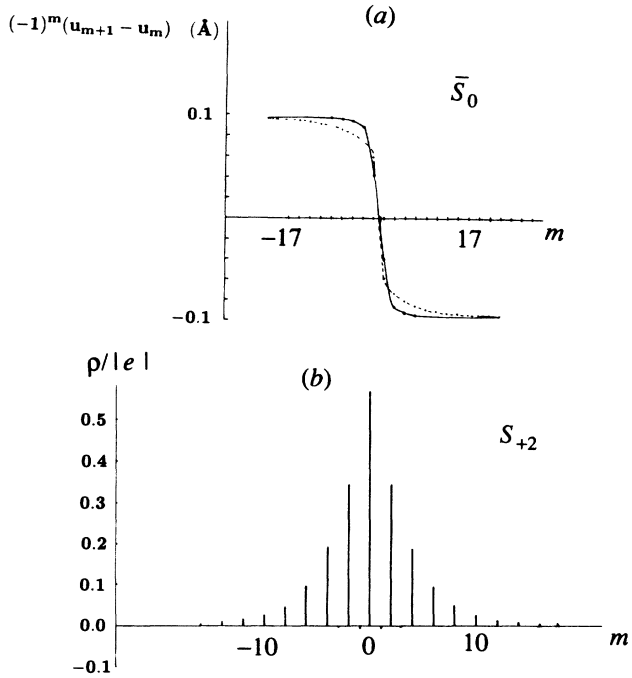

FIG. 4. (a) The relative displacements for a neutral antisoliton $\bar{S}_0$ (dashed curve) together with that obtained using the hyperbolic-tangent assumption (solid curve). (b) The internal charge structure of a doubly charged soliton S_{2+}.

configuration coordinates around the defect together with the hyperbolic-tangent curve from the variational approach. The agreement is seen to be fair although some modifications appear, which thus must be ascribed discreteness and anharmonicity.

In Table I we have collected the calculated total energies using the two approaches for different charges of the polymer together with those for the undistorted polymer of the same charge. In agreement with the hyperbolic-tangent form to be a reasonable approximation the energies of the first approach are only slightly larger than those of the second approach.

Compared with the simplest SSH model for *trans*-polyacetylene[8,9] we notice the very important difference that singly charged solitons have larger energies than the similarly charged undistorted system. This is also found in the harmonic model for polyyne,[13–15] but in our approach the formation energy of a soliton is larger than in the harmonic model. We can understand this as a result of the anharmonic term in H_σ: For a distortion in which $|u_n|$ in a smaller region is decreased compared with the optimal value $|u_{(0)}|$ the SSH model predicts that there will be a competition between H_σ which favors any value of $|u_n|<|u_{(0)}|$ and H_π which disfavors it. But for the present anharmonic model both parts disfavor values of $|u_n|<0.02$ Å $\simeq 0.4u_{(0)}$, and singly charging the polymer by simply adding an electron to the conduction bands or removing it from the valence bands is accordingly energetically favored . On the other hand, Table I shows that doubly charged solitons are energetically favored com-

TABLE I. Total energies (in eV) for a polymer of charge $Q|e|$. In the variational approach (labeled "var.") a soliton is assumed being of hyperbolic-tangent form and d gives the center of the soliton. In the self-consistent approach (labeled "scf") no assumption of the solitonic shape is made. For comparison the last column (labeled "undist.") gives the energies of the undistorted polymer of the same charge. The numbers in parentheses are the binding energies of the soliton, i.e., the total energies of the undistorted system of charge $Q|e|$ minus that of the soliton of the same charge. The binding energy is positive (negative) for stable (metastable) solitons. In comparing solitons of different charges one should compare the binding energies per charge.

Q	$d=0.00$ (var.)	$d=0.25$ (var.)	$d=0.50$ (var.)	scf	undist.
+2	1.62	1.64	1.70	1.56	1.85
	(0.23)	(0.21)	(0.15)	(0.29)	
+1	1.45	1.47	1.53	1.38	0.92
	(−0.53)	(−0.55)	(−0.61)	(−0.46)	
0	1.28	1.30	1.35	1.21	0.00
	(−1.28)	(−1.30)	(−1.35)	(−1.21)	
−1	1.10	1.13	1.18	1.04	0.56
	(−0.54)	(−0.57)	(−0.62)	(−0.48)	
−2	0.93	0.95	1.01	0.86	1.13
	(0.20)	(0.18)	(0.12)	(0.27)	

pared with the undistorted system of the same charge. Finally, as has been argued elsewhere,[7,15] the soliton-induced gap state does not appear exactly at midgap due to the presence of the next-nearest-neighbor interactions, although the shift away from midgap is very small (<0.01 eV).

We show in Fig. 4(b) the internal charge structure (defined as the charge density of the actual system minus that of the neutral, undistorted, dimerized system) for a doubly positively charged soliton. The next-nearest-neighbor interactions cause small but finite (negative) components to show up between the large (positive) components on every second site. It is moreover seen that the orbital is spread out over about 10–20 C units, whereas the soliton-induced orbital for *trans*-polyacetylene typically extends over 20–40 CH units.[57] Finally, some deviations from the sech^2 dependence (as the harmonic continuum approximation gives) are also noticed; due to the small width of the soliton, a better description might be a power law as has been suggested for solitons of vanishing width.[7]

Rice *et al.*[13,14] have also used a hyperbolic-tangent ansatz for the shape of solitons. However, due to their lack of reasonable parameters they find a somewhat larger optimized value of L, around 2.4 in the continuum limit and around 2.0 for a discrete chain.

Recently Williams[16] applied a semiempirical Hartree-Fock method on finite HC_nH molecules. Due to the Hartree-Fock approximation the gap is found to be large (5.5–8.5 eV) but based on some additional semiempirical CI (configuration-interaction) calculations he estimated the correct value to be 2.5 eV. He examined neutral and charged solitons by optimizing all internal coordinates. His results indicate $L=2$–3 and $u_{(0)}=0.039$ Å, of which especially the latter agrees well with our values. For unknown reasons his soliton-induced gap state appears for some of the solitons far from the midgap position.

3. *Polarons*

Within the self-consistent approach we used as an initial ansatz

$$v_n=(-1)^n(\Delta_0-K_\theta v_F\{\tanh[K_\theta(n+by_\theta)] -\tanh[K_\theta(n-by_\theta)]\}) \tag{21}$$

with

$$\Delta_0=4\alpha_1 u_{(0)}\ ,$$
$$K_\theta=\frac{2t_1}{\Delta_0}\sin\theta\ ,$$
$$y_\theta=\frac{2t_1}{\Delta_0\sin\theta}\tanh^{-1}[\tan(\theta/2)]\ , \tag{22}$$
$$\theta=\frac{h+n}{N}\frac{\pi}{2}\ .$$

Here, h (n) is the number of holes (electrons) in the lower (upper) polaron-induced gap orbital (each being 0, 1, 2, 3, or 4). For $v_f=2t_1$ and $b=1$, Eqs. (21) and (22) correspond to the exact solutions in the harmonic continuum limit, as demonstrated by Rice *et al.*[13,14] For other values of v_f and b the amplitude and the length, respectively, of the polaron are varied.

Using different initial assumptions for v_f and b we found a variety of (meta)stable polarons for different spin and/or charge. In Fig. 5 we depict schematically those with the lowest total energies by showing the valence- and conduction-band edges plus the polaron-induced states together with the occupancies of the latter. Also shown is the binding energy defined as the total energy of the undistorted polymer minus that of the polaronic distorted polymer both having the same charge and spin. The binding energy is thus positive (negative) when the

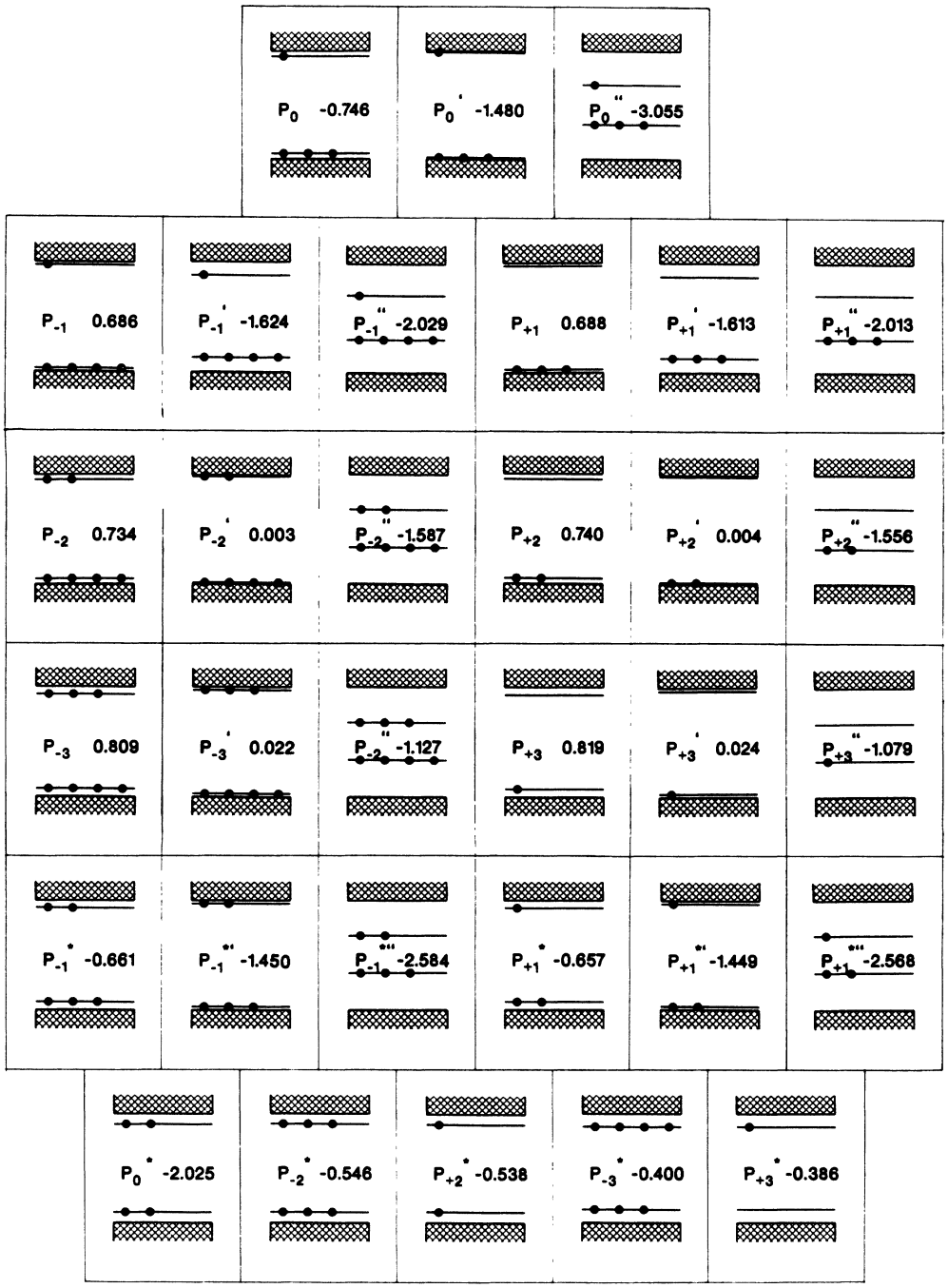

FIG. 5. Various (meta)stable polarons in schematic form. For each diagram the lower and upper cross-hatched area represents the valence- and conduction-band region, respectively, whereas the horizontal lines in the gap represent the polaron-induced levels (their positions are drawn to scale) together with their occupation (one circle corresponds to one electron; each level can contain at most four electrons). The label and the binding energy (in eV) are included in each diagram.

polaron has a lower (higher) total energy that the undistorted chain.

In discussing the results of Fig. 5 we first mention the finding of three modifications for each type of polaron, which we denote according to their binding energy (E_b) as P, P', and P'', respectively, such that $E_b(P) > E_b(P') > E_b(P'')$. In Fig. 5 we notice that otherwise identical polarons but with opposite charges have slightly different binding energies and positions of the induced levels. This is due to the next-nearest-neighbor interactions, which break the electron-hole symmetry.[15]

The formation energy (the negative of the binding energy) of a polarexciton (P_0) is strongly reduced by the anharmonicity (it becomes here roughly Δ_0 whereas it is $1.81\Delta_0$ in the harmonic continuum limit). Hence, the formation energy of two polarexcitons is

$2[-E_b(P_0)]=1.49$ eV (see Fig. 5) and is thus smaller than that of a neutral soliton-antisoliton pair $[-2E_b(S_-)=2.42$ eV; see Table I]. Accordingly, the decay of two polarexcitons into a soliton-antisoliton pair is here prevented, whereas in the simplest harmonic approximation it is possible. In contrast, two polarexcitons of type P_0^* or four polarexcitons can decay into a soliton-antisoliton pair.

The most important result here is the stabilization of a polaron lattice in comparison with a soliton lattice at least in the dilute limit. The anharmonicity of H_σ is the reason for this difference. This leads to a local energy maximum of E_σ for $u_n=0$ in contrast to a local energy minimum in the harmonic approximation, and thus, all structures with a larger number of sites with small values of $|u_n|$ become less favored.

As an example of a weakly doped polymer chain we consider a very long chain of charge $\pm 12|e|$. Using the numbers of Fig. 5 and Table I it is now straightforward to calculate that the total energy of twelve well-separated singly charged polarons $P_{\pm 1}$ is 8.3 eV below that of the undistorted chain. Also six doubly charged polarons (4.4 eV) and four triply charged polarons (3.3 eV) have lower total energies. These three configurations have furthermore all lower total energies than the lowest total energy of a chain with solitons. This is, on the other hand, found for three well-separated pairs of well-separated quadruply charged soliton-antisoliton pairs and is lower (1.3 eV) than the total energy of the undistorted chain. Also configurations involving some of the excited metastable polarons have lower total energies than the undistorted polymer as can be seen by examining Fig. 5. This complexity of possible metastable states makes the dynamics of the localization process of injected charges nontrivial.

The relative displacements (order parameter) and the internal charge structure of some polarons are shown in Fig. 6. As usual the polarons can to some extent be idealized as a bound state of a soliton and an antisoliton. Compared with the polaron profiles as found within the harmonic approximation both larger depths and larger tails are here observed, whereas each half part of the polaron seems steeper.

In comparing our results for polarons with those of Rice *et al.*[13,14] the richness of the (meta)stable polarons found in the anharmonic approximation is striking. All types of polarons already present in the harmonic approach are favored by the anharmonicity. Moreover, the present approach predicts two singly charged polarons to have lower total energy than the doubly charged soliton in contrast to the findings of Rice and co-workers. The results of the semiempirical Hartree-Fock calculations by Williams[17] are in qualitative agreement with those of Rice *et al.* and we will not comment on them further.

B. Bending chains and twistons

Although the stability of twistons for "conventional" sp^2-bonded conjugated polymers is believed to be due to interchain interactions,[18] we will examine here twistons in an isolated chain of the "unconventional" *sp*-bonded conjugated polyyne polymer. We believe the results to be of relevance when understanding the nature of the twistons. In analyzing the twistons we have only used the variational approach.

First of all we define an arbitrary plane which as assumed to contain the nuclei of the undistorted chain as well as those of the distorted system. **N** is a normal to this plane. We will let θ_n be the bond angle of the *n*th carbon atom. θ_n is assumed positive (negative) when the vector $(\mathbf{r}_{n-1}-\mathbf{r}_n)\times(\mathbf{r}_{n+1}-\mathbf{r}_n)$ is parallel (antiparallel) to **N** (we ignore the case of $\theta_n=\pm 180°$ for which the sign is irrelevant). Here, $\mathbf{r}_n$ is the position of the *n*th carbon atom. We can then consider two different highly symmetric types of excitations; one where the chain is bending locally (i.e., all $\theta_n \neq 180°$ have the same sign), and one

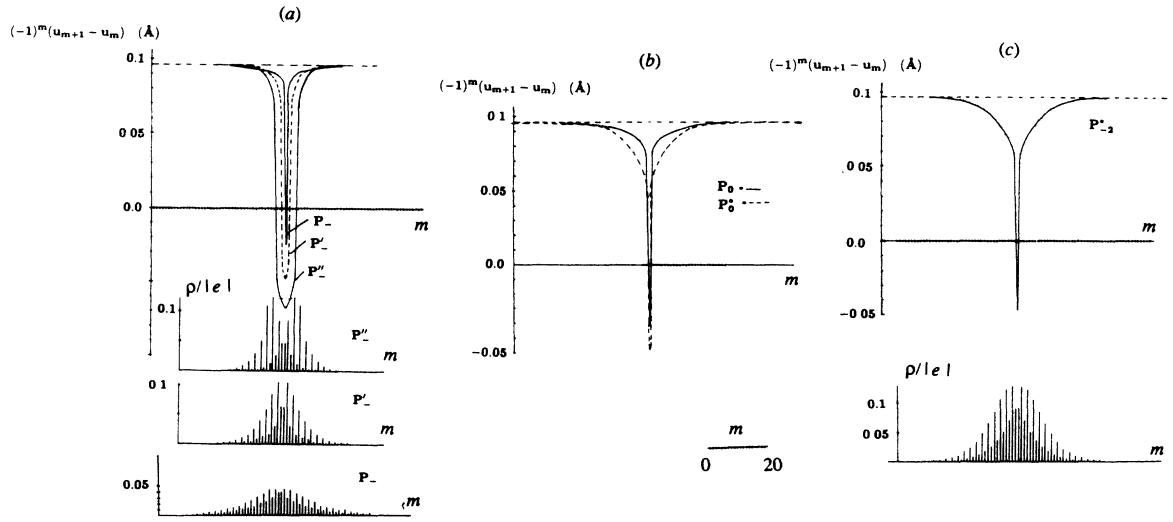

FIG. 6. The relative displacements for some selected polarons of Fig. 5: (a) P_{-1}, P'_{-1}, and P''_{-1}; (b) P_0 and P_0^*; and (c) P^*_{-2}. In (a) and (c) the internal charge structures of the polarons are also shown, and in (b) we show for reference a small scale showing the length of 20 sites.

where the chain has a local zigzag arrangement (i.e., the $\theta_n \neq 180°$ have alternating signs). We will *model* these by

$$\phi_n = a\,\mathrm{sech}\left[\frac{n+d}{L}\right] \tag{23}$$

in the first ("bent") case, and

$$\phi_n = (-1)^n a\,\mathrm{sech}\left[\frac{n+d}{L}\right] \tag{24}$$

in the second ("zigzag") case. We have introduced

$$\phi_n = 180° - \theta_n \ . \tag{25}$$

Many other related excitations can be proposed. For instance, excitations where the sign of ϕ_n is changing every mth n value are possible. We point out that in our model below we cannot distinguish between these different types of excitations.

We write the total Hamiltonian as a sum of a tight-binding term $H_\pi = H_\pi^\pi + H_\pi^\sigma$ describing the π orbitals and the π-generated σ orbitals and a remainder H_σ. In the limit $\phi_n = 0$ the energies of the π orbitals and the π-generated σ orbitals become degenerate. The hopping integrals of H_π for the longer carbon-carbon bonds between atom n and atom $n-1$ are modeled through

$$t_{-1}^\sigma = 1.78\ \mathrm{eV} + 10^{-5}(|\phi_{n-1}| + |\phi_n|)^2\ \mathrm{eV/deg^2}\ ,$$
$$t_{-1}^\pi = 1.78\ \mathrm{eV} + 10^{-5}(|\phi_{n-1}| + |\phi_n|)^2\ \mathrm{eV/deg^2}\ , \tag{26}$$

and those of the shorter carbon-carbon bonds between atom n and atom $n+1$ through

$$t_{+1}^\sigma = 2.60\ \mathrm{eV} + 0.01\left[\cos\left[\frac{|\phi_{n+1}| + |\phi_n|}{24°} \times 180°\right] - 1\right]\mathrm{eV}\ ,$$
$$t_{+1}^\pi = 2.60\ \mathrm{eV} + 0.03\left[\cos\left[\frac{|\phi_{n+1}| + |\phi_n|}{50°} \times 180°\right] - 1\right]\mathrm{eV}\ , \tag{27}$$

which for $\phi_n = \phi$ const becomes identical to Eq. (8). Next-nearest-neighbor interactions are neglected.

H_σ is written as

$$H_\sigma = (5 \times 10^{-4}\ \mathrm{eV/deg^2}) \sum_n \phi_n^2\ . \tag{28}$$

For the undistorted polymer the top of any of the valence bands is at $-(t_{+1} - t_{-1})$ and the bottom at $-(t_{+1} + t_{-1})$. Assuming all ϕ_n to have the same value ($=\phi$) we see from Eqs. (26) and (27) that for both the σ and the π band t_{-1} (t_{+1}) is an increasing (decreasing) function of ϕ for small values of ϕ. Thus, both the top and the bottom of the valence band are shifted towards higher energies as a function of ϕ. Therefore, both H_π and H_σ favor the high-symmetry structure for the neutral polymer. Interpreting the excitation of Eqs. (23) and (24) as locally creating a part of the chain with an effective $\phi \neq 0$ the electronic orbitals of this region will in general be above those of the rest of the chain. Similarly, the orbitals derived from the conduction band will be below those of the rest of the conduction band. Therefore, compared with the undistorted system it will cost less energy to remove electrons from or add electrons to the distorted system. Accordingly, for both the positively and negatively charged polymer there will be a competition between H_π which favors a distortion, and H_σ, which favors the undistorted structure.

Our calculations showed, however, that for all singly, doubly, triply, and quadruply positively and negatively charged polymers the undistorted chains have the lowest total energy. As can be shown,[7] a twiston does not lead to (near-) midgap states, and the charged twistonic distorted polymers are therefore not stabilized by their appearance as are some charged solitonic distorted polymers. We believe this lack to be the reason for the instability of twistons. Furthermore, this lack makes the interaction between solitons and twistons suggested by Brazovsky and Kirova[18] only very weak.

V. CONCLUSIONS

We have reported results of first-principles calculations on periodic carbon chains with alternating bond lengths. The results were used in providing parameters for model Hamiltonians with tight-binding descriptions (H_π) of the two uppermost valence bands and simple analytical forms (H_σ) of the remaining parts of the total energy.

For linear chains we found such models to be adequate, and the parameters to vary less than roughly 10% for reasonable variations in the unit-cell lengths. It was argued that for larger variations in the unit-cell length (which might be the case near defects) extra on-site terms depending on nearest-neighbor bond lengths should be included in H_π, although that was not done in the present work.

Using two different approaches (a variational and a self-consistent) we examined solitons and polarons. Due to the existence of anharmonic terms in H_σ, polarons were favored compared with solitons. Moreover, the ground state of a singly charged polymer corresponds to a chain containing a polaron, and for a multiply charged polymer the system prefers a structure of separated, weakly interacting, singly charged polarons (a polaron lattice). Therefore, the model predicts an increased ESR signal upon doping. Furthermore, a very rich spectrum of different (meta)stable polarons was predicted, also due to the anharmonic terms in H_σ.

Although the dimerization amplitude for *sp*-bonded polyyne is larger than that for sp^2-bonded conjugated polymers, we believe that anharmonic terms could be present also for the latter. These could lead to larger dimerization energies (see, e.g., Ref. 58). Moreover, they can lead to a large number of gap states due to the existence of different (meta)stable polarons (cf. Fig. 5) and make interpretations of optical-absorption spectra of doped polymers more complicated than is usually assumed. The existence of anharmonicities for polyyne can, for instance, be examined by enhanced isotope effects (^{12}C versus ^{13}C) in Raman and infrared modes.

By parametrizing results of calculations on zigzag

chains, we suggested a model that could be used in qualitatively analyzing the analogues of the twistons which have been proposed for planar conjugated polymers.[18] The lack of (near) mid-gap states made the twistons unstable, and we predict therefore similar instabilities to show up for other twistonic distorted conjugated polymers. However, interchain interactions might stabilize them as has been proposed.[18]

ACKNOWLEDGMENTS

One of us (M.S.) acknowledges the hospitality of Professor P. Ziesche, Technical University of Dresden, where this work was completed. We thank furthermore Professor G. Lehmann for his continuous interest. Finally, M.S. was partly supported by the Danish Natural Science Research Council.

---

*Present address.

†Permanent address: Institute of Physics, Czechoslovak Academy of Sciences, Prague, Czechoslovakia.

[1]C. K. Chiang, C. R. Fincher, Jr., Y. W. Park, A. J. Heeger, H. Shirakawa, E. J. Louis, S. C. Gau, and A. G. MacDiarmid, Phys. Rev. Lett. **39**, 1098 (1977).

[2]*Proceedings of the International Conference on the Physics and Chemistry of Low-dimensional Synthetic Metals, 1984* [Mol. Cryst. Liq. Cryst. **117–121** (1985)].

[3]*Proceedings of the International Conference on Science and Technology of Synthetic Metals, 1986* [Synth. Met. **17–19** (1987)].

[4]*Proceedings of the International Conference on Science and Technology of Synthetic Metals, 1988* [Synth. Met. **27–29** (1988–1989)].

[5]S. Roth and H. Bleier, Adv. Phys. **36**, 385 (1985).

[6]H. W. Streitwolf, Phys. Status Solidi B **127**, 11 (1985).

[7]M. Springborg, H. Kiess, and P. Hedegård, Synth. Met. **31**, 281 (1989).

[8]W. P. Su, J. R. Schrieffer, and A. J. Heeger, Phys. Rev. Lett. **42**, 1698 (1979).

[9]W. P. Su, J. R. Schrieffer, and A. J. Heeger, Phys. Rev. B **22**, 2099 (1980); B **28**, 1138 (E) (1983).

[10]V. I. Kasatochkin, A. M. Sladkiv, Y. P. Kudryatsev, N. M. Popov, and V. V. Korschak, Dokl. Akad. Nauk SSSR **177**, 358 (1967).

[11]K. Akagi, M. Niguchi, and H. Shirakawa, Synth. Met. **17**, 557 (1987).

[12]M. Springborg, J. Phys. C **19**, 4473 (1986).

[13]M. J. Rice, S. R. Phillpot, A. R. Bishop, and D. K. Campbell, Phys. Rev. B **34**, 4139 (1986).

[14]S. R. Phillpot, M. J. Rice, A. R. Bishop, and D. K. Campbell, Phys. Rev. B **36**, 1735 (1987).

[15]J. Málek, S. L. Drechsler, E. Heiner, and R. Kahnt, Phys. Status Solidi B. **147**, 281 (1988).

[16]G. R. J. Williams, J. Phys. C **21**, 1971 (1988).

[17]G. R. J. Williams, Synth. Met. **31**, 61 (1989).

[18]S. A. Brazovsky and N. N. Korova, Solid State Commun. **66**, 11 (1988).

[19]M. Springborg and O. K. Andersen, J. Chem. Phys. **87**, 7125 (1987).

[20]M. Springborg, J. Chim. Phys. **86**, 715 (1989).

[21]P. Hohenberg and W. Kohn, Phys. Rev. **136**, B864 (1964).

[22]W. Kohn and L. J. Sham, Phys. Rev. **140**, A1133 (1965).

[23]A. R. Williams and U. von Barth, in *Theory of the Inhomogeneous Electron Gas,* edited by S. Lundqvist and N. H. March (Plenum, New York, 1983).

[24]U. von Barth and L. Hedin, J. Phys. C **5**, 1629 (1972).

[25]M. Springborg, Phys. Rev. B **33**, 8475 (1986).

[26]M. Springborg, Phys. Scr. T **13**, 306 (1986).

[27]M. Springborg, Phys. Rev. B **37**, 1218 (1988).

[28]M. Kertész, J. Koller, and A. Ažman, J. Chem. Phys. **68**, 2779 (1978).

[29]M. Kertész, J. Koller, and A. Ažman, Phys. Rev. B **19**, 2034 (1979).

[30]A. Karpfen, J. Phys. C. **12**, 3227 (1979).

[31]H. Teramae, T. Yamabe, and A. Imamura, Theor. Chim. Acta (Berlin) **64**, 1 (1983).

[32]K. Tanaka, M. Okada, T. Koike, and T. Yamabe, Synth. Met. **31**, 181 (1989).

[33]J. Ashkenazi, W. E. Pickett, H. Krakauer, C. S. Wang, B. M. Klein, and S. R. Chubb, Phys. Rev. Lett. **62**, 2016 (1989); **63**, 1539 (E) (1989).

[34]J. W. Mintmire and C. T. White, Phys. Rev. Lett. **50**, 101 (1983).

[35]J. W. Mintmire and C. T. White, Phys. Rev. B **28**, 3283 (1983).

[36]J. Ashkenazi, W. E. Pickett, B. M. Klein, H. Krakauer, and C. S. Wang, Synth. Met. **21**, 301 (1987).

[37]J. W. Mintmire and C. T. White, Phys. Rev. B **35**, 4180 (1987).

[38]J. W. Mintmire and C. T. White, Int. J. Quant. Chem. Symp. **21**, 131 (1987).

[39]P. Vogl and D. K. Campbell, Phys. Rev. Lett. **62**, 2012 (1989).

[40]L. Ye, A. J. Freeman, D. E. Ellis, and B. Delley, Phys. Rev. B **40**, 6277 (1989).

[41]M. Springborg, J. -L. Calais, and O. Goscinski, unpublished.

[42]A. Karpfen and J. Petkov, Solid State Commun. **29**, 251 (1979).

[43]A. Karpfen and J. Petkov, Theor. Chim. Acta (Berlin) **53**, 65 (1979).

[44]T. Yamabe, K. Tanaka, H. Teramae, K. Fukui, A. Imamura, H. Shirakawa, and S. Ikeda, J. Phys. C **12**, L257 (1979).

[45]A. Karpfen and R. Höller, Solid State Commun. **37**, 179 (1981).

[46]T. Yamabe, T. Matsui, K. Akagi, K. Ohzeki, and H. Shirakawa, Mol. Cryst. Liq. Cryst. **83**, 125 (1982).

[47]S. Suhai, Phys. Rev. B **27**, 3506 (1983).

[48]S. Suhai, Chem. Phys. Lett. **96**, 619 (1983).

[49]H. Teramae, T. Yamabe, and A. Imamura, J. Chem. Phys. **81**, 3564 (1984).

[50]J. L. Brédas, M. Dory, and J. M. André, J. Chem. Phys. **83**, 5242 (1985).

[51]J. C. Schug, R. D. Reid, A. C. Lilly, and R. W. Dwyer, Chem. Phys. Lett. **128**, 5 (1986).

[52]H. O. Villar and M. Dupuis, Chem. Phys. Lett. **142**, 59 (1987).

[53]H. O. Villar, M. Dupuis, J. D. Watts, G. J. B. Hurst, and E. Clementi, J. Chem. Phys. **88**, 1003 (1988).

[54]R. H. Baughman, S. L. Hsu, G. P. Pez, and A. J. Signorelli, J. Chem. Phys. **68**, 5405 (1978).

[55]C. S. Yannoni and T. C. Clarke, Phys. Rev. Lett. **51**, 1191 (1983).

[56]D. K. Campbell and A. R. Bishop, Nucl. Phys. B **200**, 297 (1982).

[57]D. S. Boudreaux, R. R. Chance, J. L. Brédas, and R. Silbey, Phys. Rev. B **28**, 6927 (1983).

[58]M. Springborg, Synth. Met. **28**, D527 (1989).